17th World Conference on Earthquake Engineering, 17WCEE
Sendai, Japan - September 13th to 18th 2020

Real-time Hybrid Experiment of "CaSS" for Function Separated Bridge

N. Yamazaki[1], J. Dang[2], Y. Akiike[3] , M. Ishiyama[4], Y. Someya[5]

[1] *Research and Development Engineer, Technical Research Laboratory, NIPPON CHUZO K.K., n_yamazaki@nipponchuzo.co.jp*
[2] *Assistant Professor, Dept. of Civil & Environment Engineering, Saitama University, dangji@mail.saitama-u.ac.jp*
[3] *Design Engineer, NEXCO-West Consultants Co., Ltd., y.akiike@w-nexco-consul.co.jp*
[4] *Design Engineer, Engineering Division, Design Dept., NIPPON CHUZO K.K., m_ishiyama@nipponchuzo.co.jp*
[5] *Design Engineer, Engineering Division, Design Dept., NIPPON CHUZO K.K., y-someya@nipponchuzo.co.jp*

Abstract

In recent years, many bridge structures were damaged due to large earthquakes such as Tohoku Earthquakes and Kumamoto Earthquakes. The effects and loads on bridges are with great uncertainty and the hazards that might be experienced are difficult to predict. The probability of having an earthquake beyond the design code must not be ignored and the damages and seismic risks must be mitigated by considering the said probability. In this study, as shown in Fig.1, the concept of Function Separated Bridge was introduced to control the unfunctional time due to damage in key components such as rubber bearings.

For Function Separated Bridge, the multiple functions are dispersed into individual damper or bearing in which even if one of the devices was damaged the whole system will not lose its total functionality. In this study, concept of function decentralized structure was brought forward with a model consisting of Sliding bearing (BPB) (to support vertical load), Cylinder damper (NES-D) (to absorb deformation such as temperature expansion and contraction in girder), Shear Panel damper (SPD) (to absorb earthquake energy) and High Damping Rubber Bearing (HDRB) (to provide horizontal restoring force). All materials and methods that have been used in the work must be stated clearly.

It was found out that the main destruction mode of the Function Separated Bridge is when the SPD of the abutment breaks first before the HDRB of the piers. According to earthquake risk assessment, the risk of Function Separated Bridge is about the half of the traditional isolated bridge. It was also found that Function Separated Bridge is economical and can quickly be restored by a combination of low cost and easy-to-install bearings considering the earthquake risk, and it contributes to restoration of the damaged area by suppressing loss.

In order to apply Cylinder and Shearing-panel Series (CaSS) to an actual bridge, it is necessary to grasp the influence of the dynamic restoring force characteristics of the seismic isolation device on the seismic response of the entire structure. Large scale equipment and facilities are required to obtain the real earthquake response of large structures such as civil engineering structures. In addition, a real-time loading test is desirable to verify the damping performance of a series of damping damper whose response depends on the ground motion speed.

In this study, the performance of the "CaSS" shown in Fig.2 was verified. The "CaSS" has a shear panel damper and a cylinder damper connected in series. There are two types of performance verification methods: constant amplitude loading using a sine wave and hybrid experiments. The real-time hybrid experiment used a system that was developed to evaluate the behavior of the entire structural system through a loading test using only "CaSS" and a dynamic response analysis of other members. Through these experiments, we investigated the seismic response characteristics of the seismic isolated bridge considering the actual seismic response of "CaSS".

Keywords: Function Separated Bridge, Shear Panel Damper, Cylinder Damper, Real-time Experiment, Risk Assessment

1. Introduction

The 2011 Off the Pacific Coast of Tohoku Earthquake (M 9.0; also called as the Great East Japan Earthquake), which occurred on March 11, 2011, was the largest earthquake ever recorded in Japan and its surrounding area at that time. Due to its extreme ground motion, a massive tsunami followed, which caused enormous damage and a serious social problem – the accident at the Fukushima Daiichi Nuclear Power Plant. In the Japan Society of Civil Engineers (JSCE), the Follow-up Committee for the Great East Japan Earthquake, Special Task Committee on Nuclear Safety Civil Engineering Technology was established in response to these circumstances and compiled "Recommendations on Criteria for Seismic and Tsunami Resistant Performance for Nuclear Power Generation (Civil Engineering Viewpoint)." [1]. In those Recommendations, the framework of design for earthquakes and tsunamis and risk management for achieving the goal of nuclear safety were reviewed, and the concept of "anti-catastrophe performance" was added to the conventional concept of "safety." As used here, "safety" means a condition in which a nuclear power plant will not suffer serious damage under basic earthquake ground motion or an ensuing tsunami. "Anti-catastrophe performance" is defined as performance that sufficiently minimizes the possibility that a catastrophic condition will occur immediately in case "safety" was impaired, that is, even in case of conditions that exceed the basic earthquake ground motion or tsunami.

Seismic design of bridges is also carried out based on the concepts of anti-catastrophe performance and resilience. [2] etc. In the Seismic Design Standards Subcommittee of the JSCE's Earthquake Engineering Committee, the concept of "anti-catastrophe performance" was arranged in seismic design. There, "anti-catastrophe performance" is defined as "the quality that a structures do not fall into a catastrophic condition, as units or as a system, even in events that had not been assumed in the stage of design in the narrow sense." The phrase "design in the narrow sense" is considered to mean "confirming by verification that a structure satisfies performance requirements for Level 1, Level 2, etc. design earthquake motion." For example, in the Kumamoto Earthquakes of 2016, traffic on an expressway with a high degree of importance was temporarily blocked by the collapsed over-bridge with a low degree of importance. The concept of anti-catastrophe performance in seismic design considers not only seismic performance verification of unit structures, but also the influence of those structures on their surroundings. For this reason, clarification of the functions of structures and devices and their performance is important.

Seismic isolation rubber bearings have a variety of functions; in addition to bearing, movement and rotation of vertical and horizontal force, these also include generation of damping force and restoring force. From the viewpoint of bearing maintenance and control, the top surface of the substructure should be as simple as possible. However, in cases where it is difficult to assess the object functions due to deterioration of the members with age, etc., and when the anti-catastrophe performance of the whole structure and the resilience of the traffic system are considered, distribution of risks and functions over multiple devices will be considered effective. (In the following, this approach is referred to as a "function separated bridge.") Moreover, describing the purpose of individual devices narrowly will clarify their performance, thereby contributing to improved design reliability.

Therefore, the authors studied function separated bridge focusing on bearings, where bridge functions are concentrated. [3] etc. As a feature of this type of system, from the viewpoints of anti-catastrophe performance and deterioration with age, the functions under normal conditions and during an earthquake are distributed among various devices. Even in the unlikely event of conditions that exceed the design ground motion, the possibility that the bridge will immediately reach a dangerous state is sufficiently minimized by inducing damage in certain designated members. In the present research, the researchers conducted a performance verification of a device (Cylinder and Shearing-panel Series: CaSS) consisting of a cylinder type viscous damper (NES-D), which displays velocity dependency, and a steel lens-type shear panel damper (LSD) in series as a function separated bridge from the viewpoints of anti-catastrophe performance and deterioration with age. Concretely, first, a sine-wave reverse cyclic loading test (performance confirmation experiment) was conducted in order to confirm the possibility of separating the functions that should be borne under normal conditions and during an earthquake among the respective devices. Following this, in order to verify the effect

of a series damper having complex dynamic restoring force characteristics on the whole structure, a loading experiment was conducted. The series damper and a hybrid experiment were used to assess the behavior of the system by a dynamic response analysis of other members. Also, the researchers studied the seismic response characteristics of the total isolated bridge considering the actual seismic response of the series damper. It should be noted that the conventional "function-separated bearing" is a type of bearing used to increase the degree of design freedom considering the above-mentioned "safety," wherein design ground motion is to be satisfied. Thus, the concept of this research is different from the idea of the said type of function-separated bearing.

2. Function Separated Bridge and "CaSS"

Figure 1 shows an example of the concept of a function-separated bridge. Shown in the figure is an example of a multi-span continuous girder bridge where the seismic isolation rubber bearings are used for intermediate piers and sliding bearings for vertical support at the bridge abutments. While in Fig. 2 is a cylindrical damper (NES-D) and a steel lens-type shear panel damper (LSD) which are arranged in series at the abutments. The NES-D displays the displacement velocity dependence and can be used to respond slow deformation of the girders accompanying temperature changes and live loads (hereinafter, under normal conditions) while the LSD can be used to respond to the rapid deformation that may occur during an earthquake. In LSD, damage is induced in designated members when the unlikely event of a situation exceeds the design ground motion. This enables rapid recovery of the functions of the bridge.

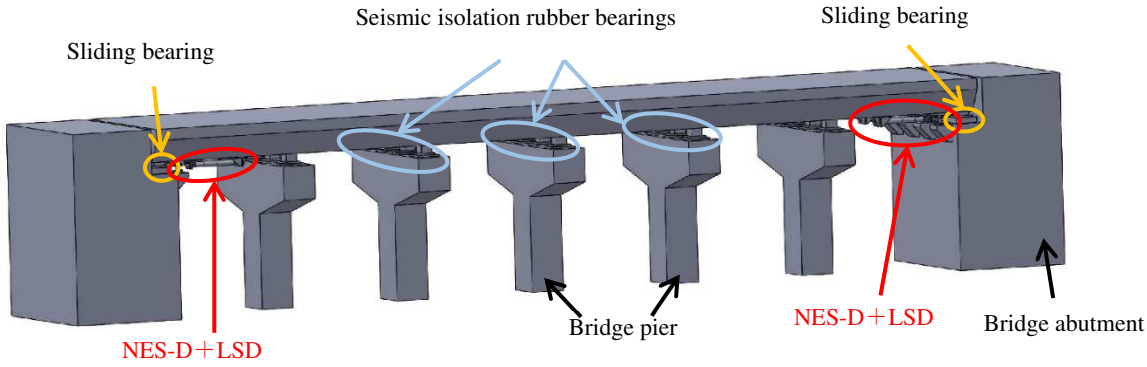

Fig. 1 – Example of concept of function separated bridge

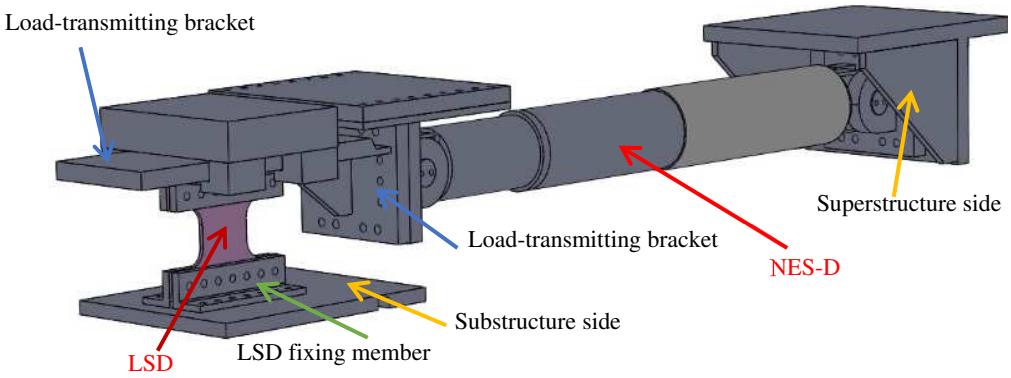

Fig. 2 – Example of "CaSS" (combination of NES-D and LSD)

3. Test Specimens

The test specimens were the NES-D with a rated load of 500 kN shown in Fig. 3 and the LY225 type 13-6.5 LSD shown in Fig. 4. These are combined in series.

As in general hydraulic devices, in the NES-D, energy is absorbed by the fluid resistance of a viscous fluid accompanying the relative motion of the cylinder and rod. In appearance, it consists of three stages. As a mechanical property of NES-D, this device generally displays displacement velocity dependence. [4]. The rated load (F) demonstrated at the rated speed of 0.5 m/s and is shown by Eq. (1). In this test, the rated load of the specimen was decided by the limitations of the test equipment.

$$F = C \times V^{\alpha} \tag{1}$$

From the equation, C is a constant, V is displacement velocity (m/s) and α is a damping coefficient (in case of this specimen, 0.1). The distance between the pins (pin distance) in the clevis parts installed at both ends of the NES-D is set considering the amount of bridge movement under normal conditions. Because the purpose of this experiment was to check the actions of the respective devices, this was set with an allowance of ±250 mm.

The LSD is a steel panel made from low yield point steel (LY225). The shape of the LSD is square with a panel width (D) and height (H) 13 times the plate thickness T (width-thickness ratio: D/T = 13). To expand the elastoplastic region, the LSD is provided with spherical concave lenses on both sides in the flat surface center area. Furthermore, the four corners of the LSD are provided with circular arc-shaped flares to relax stress concentrations. The upper and lower sides of the LSD are provided with bolt holes in a rectangular configuration for connection with the fixing members using high strength bolts. [5]. The plate thickness of this specimen is 13 mm. The panel width and height are 169 mm, and the radius of the arc-shaped flares at the four corners is 52 mm. Spherical concave areas (lenses) were machined on both surfaces in the plate center so that the minimum plate thickness was half (6.5 mm) of the original plate thickness. The yield point (σ_y) and tensile strength (σ_t) listed in the mill sheet of the specimen material were 206 N/mm^2 and 310 N/mm^2, respectively. From these values and the minimum cross-sectional area (S_{min} = 1587 mm^2) of the LSD, the yield load (P_y) and rated load (P_{rc}) of the LSD obtained from Eq. (2) and Eq. (3) were 189kN and 284kN, respectively.

$$P_y = \sigma_y / \sqrt{3} \times S_{min} \tag{2}$$

$$P_{rc} = \sigma_t / \sqrt{3} \times S_{min} \tag{3}$$

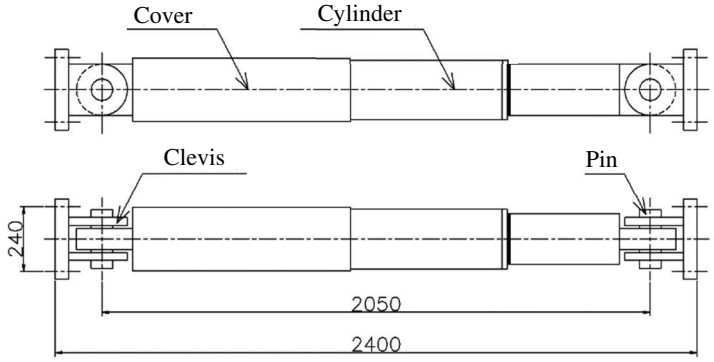

Fig. 3 – Cylinder type Viscous Damper (NES-D)

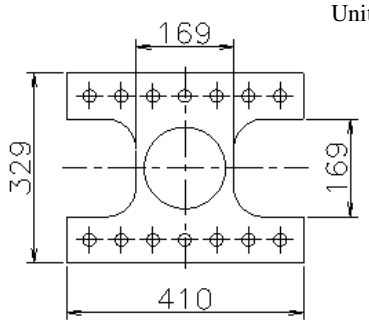

Fig. 4 – Lens type Shear Panel Damper (LSD)

The rated loads of the NES-D and LSD must be set appropriately so that deformation occurs mainly in the devices that perform the respective functions under normal conditions and during an earthquake. Although the NES-D displays velocity dependency, it has been confirmed that the load when maximum velocity is 0.1

mm/s or less is smaller than the value obtained by Eq. (1). [6]. In addition to this, a study which includes the material properties, strain hardening and other characteristics of the LSD is also necessary. However, because the purpose of the present study is to confirm actuation, the rated load of the NES-D was set at 500 kN, and that of the LSD was set at 284 kN. The performance of the respective dampers is shown in Fig. 5.

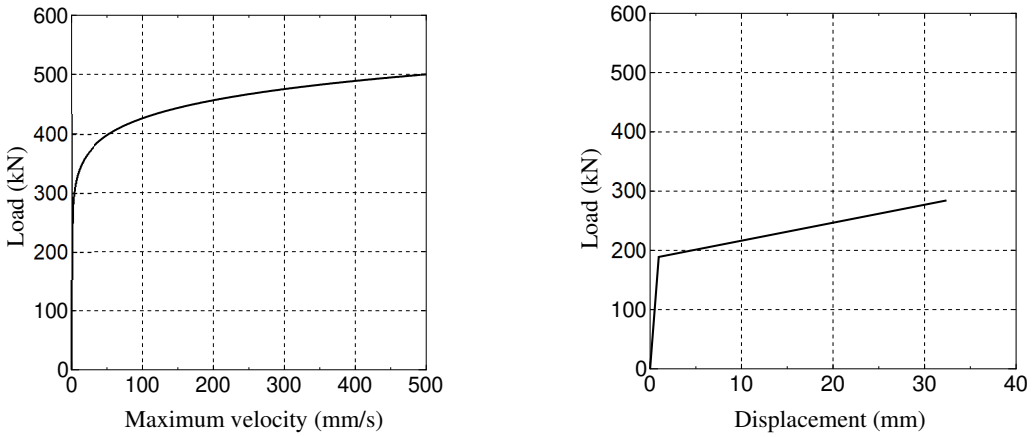

(a) Performance of NES-D (500-kN type) (b) Performance of LSD (LY225 type 13-6.5)

Fig. 5 – Performance curves of NES-D and LSD

4. Sine-Wave Reverse Cyclic Loading Experiment

4.1 Specimen Installation Condition and Test Conditions

The cyclic loading experiment was conducted with a dynamic biaxial test machine owned by NIPPON CHUZO K.K. The capacity of the test machine is 2000 kN in the vertical direction and 1000 kN in the horizontal direction. In this experiment, oscillation was applied by horizontal displacement control, while displacement in the test machine in vertical direction was fixed. Here, the combination of the NES-D and LSD shown in the example in Fig. 4 is installed in the test machine in an upside-down condition (assuming the horizontal cylinder side is the substructure and the fixing bracket side is the superstructure). Load is transmitted to the NES-D via LSD by oscillation of the horizontal cylinder.

The experimental conditions are shown in Table 1. The oscillation frequencies were 6 levels, 0.0008, 0.01, 0.05, 0.1, 0.4 and 2.0 Hz, and the horizontal displacement at all frequencies was ±20 mm. Accordingly, the respective maximum velocities was 0.1, 1.3, 6.3 12.6. 50.3 and 251.3 mm/s. The number of oscillation cycles was 10 (5 cycles only at the maximum velocity of 0.1 mm/s).

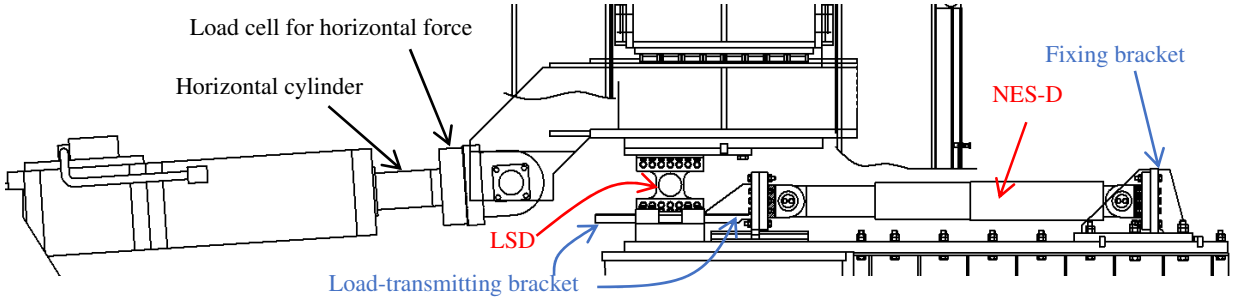

Fig. 6 – Test machine and installation condition of specimen

Photo 1 – Installation condition of specimen in test machine (overview)

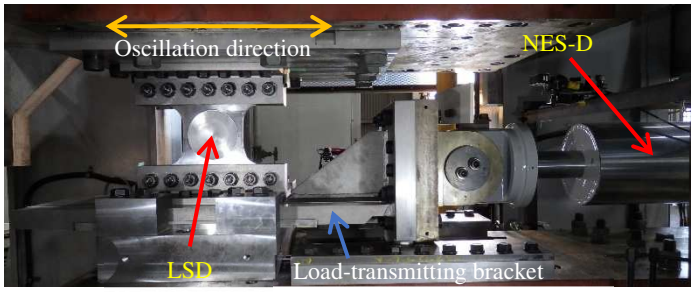

Photo 2 – Installation condition of specimen in test machine (connection between NES-D and LSD)

Table 1 – Experimental conditions (performance confirmation experiment)

Oscillation frequency (Hz)	Maximum velocity (mm/s)	Amplitude (mm)	Number of oscillation cycles	Oscillation waveform
0.0008	0.1	±20	5	Sine wave
0.01	1.3		10	
0.05	6.3			
0.1	12.6			
0.4	50.3			
2.0	251.3			

4.2 Measurement Items

In the performance checking experiment, the deformations of the NES-D and LSD and the load of the test machine were measured. The deformations of the NES-D and LSD were measured using a laser displacement sensor manufactured by KEYENCE Corporation (sensor head: IL-300 or IL-600). The measurement positions are shown in Fig. 7. The sampling period was set in the range from 1 to 1000 ms considering the maximum velocity.

The amount of deformation of the NES-D was assumed to be the difference between the displacement of the fixing bracket and the displacement of the NES-D, as shown by the green arrows in the figure. The deformation of the LSD was the difference between the upper side LSD displacement and lower side LSD displacement (shown by the orange arrows in the figure). Measurements were performed from the fixed points of the respective devices. The load of the test machine was measured by the load cell installed on the horizontal cylinder.

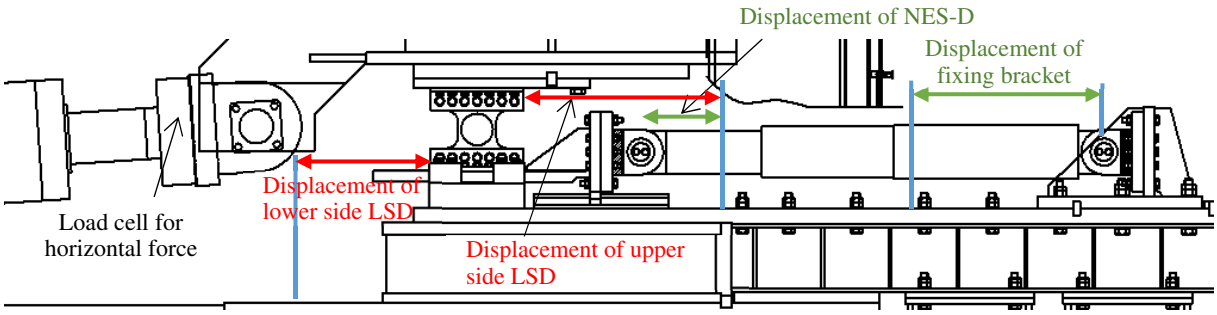

Fig. 7 – Deformation measurement positions for NES-D and LSD

4.3 Experimental Results

Figures 8 to 10 show the relationship between load and displacement obtained from the experiments at the maximum velocities of 0.1 mm/s, 1.3 mm/s and 251.3 mm/s respectively. The displacements shown on the horizontal axis in these figures are those of (a) Actuator, (b) LSD and (c) NES-D. At the maximum velocity of 0.1 mm/s, as shown in Fig. 8, the main deformation occurs in the NES-D, and the LSD is in the elastic region. This is because the maximum value of the load caused by the deformation of NES-D having a yield load of 100KN is smaller than the 184KN yield load of the LSD. The maximum load of the NES-D at the maximum velocity of 0.1 mm/s is consistent with the results of a previous report. [6]. Based on these results, it is proven that the NES-D can respond to slow velocities such as temperature changes and girder rotation under live load which are treated at normal conditions. The results for the maximum velocity of 1.3 mm/s are shown in Fig. 9. Although large deformation occurs in the NES-D, deformation also begins to appear in the LSD. This is due to the increase in maximum velocity which leads to an increase in the load of the NES-D and exceeds the 184 kN yield load of the LSD. Furthermore, if there is a continuous increase in the maximum velocity, the main deformation will shift to the LSD. The main deformation at the maximum velocity of 251.3 mm/s in Fig. 10 occurs in the LSD and no virtual deformation occurs in the NES-D. Thus, under high velocities like those during an earthquake, it is concluded that deformation can be guided to the LSD. Additionally, it may be noted that the yield load of the LSD is approximately 250kN which is higher than the one obtained by the mill sheet. This is attributed to velocity dependency. The maximum load is almost equal to the rated load of the LSD at about 300 kN. From the statement above, separation of the device functions corresponding to normal conditions and to the conditions during an earthquake is considered posible by using an appropriate combination of NES-D and LSD.

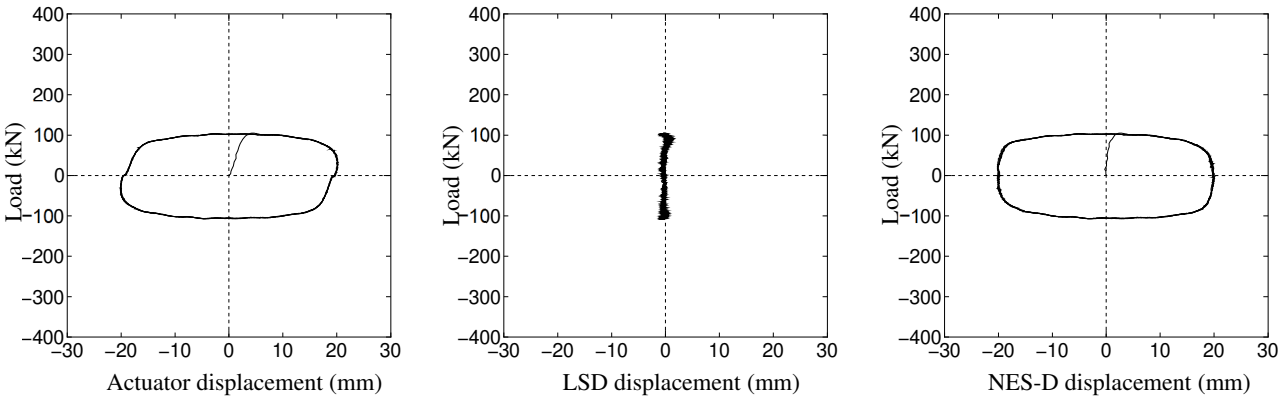

(a) Load and actuator displacement (b) Load and LSD displacement (c) Load and NES-D displacement

Fig. 8 – Experimental results for maximum velocity of 0.1 mm/s (oscillation frequency: 0.0008 Hz)

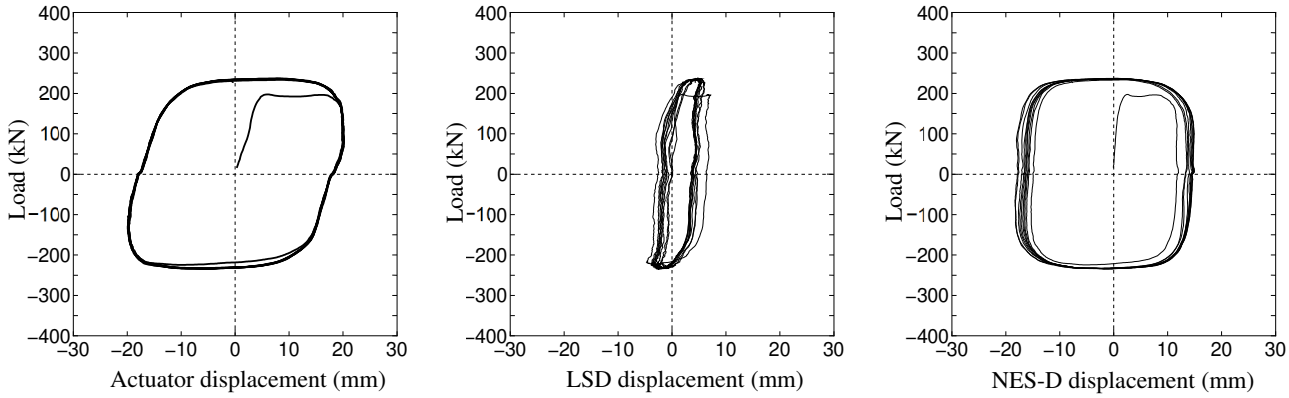

(a) Load and actuator displacement (b) Load and LSD displacement (c) Load and NES-D displacement

Fig. 9 – Experimental results for maximum velocity of 1.3 mm/s (oscillation frequency: 0.01 Hz)

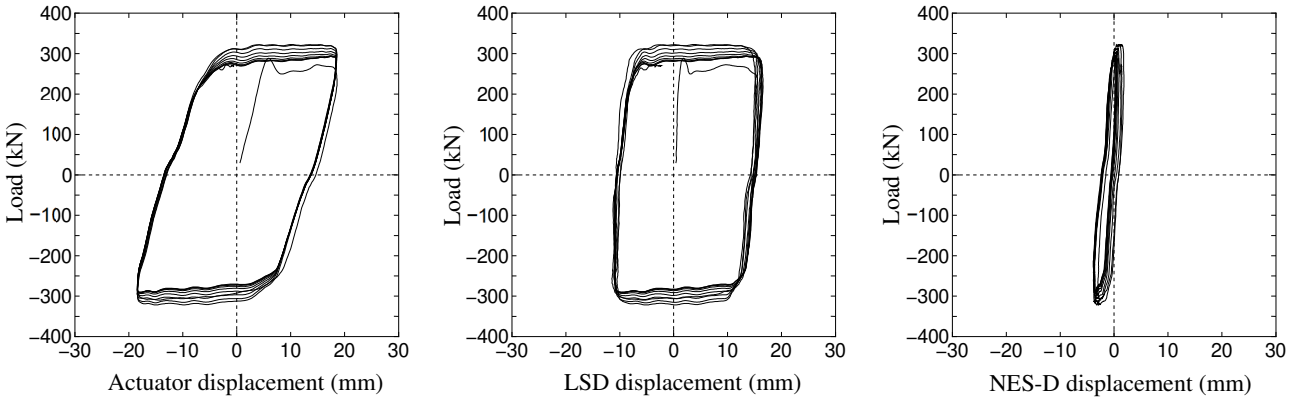

(a) Load and actuator displacement (b) Load and LSD displacement (c) Load and NES-D displacement

Fig. 10 – Experimental results for maximum velocity of 251.3 mm/s (oscillation frequency: 2.0 Hz)

5. Real Time Hybrid Simulation

The real-time hybrid simulation, as shown in Fig. 11, is a technique for investigating the seismic response of a structure as a whole by using a combination of computer-based numerical simulation and loading tests by a dynamic loading device. Two types of control systems can be used in this experiment, the system shown in Fig. 12(a), in which the main calculations are performed by a host computer (Host PC), and the system in Fig. 12(b), in which those calculations are performed by a digital signal process (DSP).

In Host PC calculations, the loading target displacement is analyzed numerically by the Host PC, and the loading device is controlled by transmitting the target displacement to the DSP, which is capable of high-speed conversion of digital and analog signals and control. As a problem in Host PC calculations, a loading delay (time lag) of approximately 7 times or more occurs due to analysis processing, etc., even in real-time loading. However, in the case of DSP calculations, in spite of the limitation on the processed data volume, there is virtually no delay due to analysis processing in real time, etc. because the numerical analysis is also performed in the DSP.

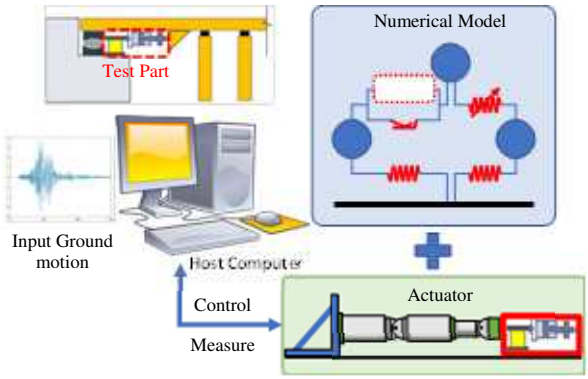

Fig. 11 – Outline of hybrid experiment

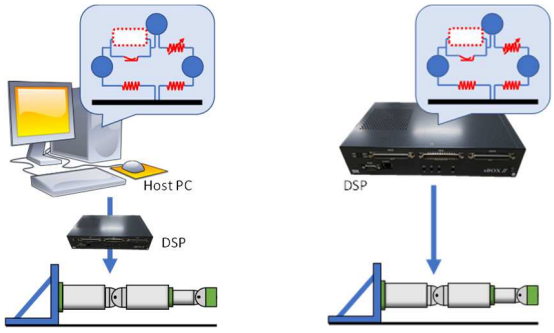

(a) Host PC calculations (b) DSP calculations

Fig. 12 – Control systems for hybrid experiment

5.1 Structural Model and Experimental Method

The assumed structural model referred to the Yamaage Bridge is located in Nasukarasuyama City, Tochigi Prefecture. Installation of a total of 10 high-damping rubber bearings (HDR), comprising 2 HDR at the top of each bridge pier, and a total of 4 sets of series dampers and sliding bearings, comprising 2 sets at the top of each abutment, was assumed. However, series dampers of the size set by the structural model could not be installed in the test device due to the limitations of that equipment. Therefore, considering a scale factor of 2.2, a series damper consisting of an LY225 type 13-6.5 LSD and a NES-D with rated resistance of 500 kN was used as the experimental specimen. This was the same as in the performance confirmation experiment.

Among the acceleration waveforms used in dynamic analysis in the seismic design of highway bridges, the input seismic motion that is used here was the NS component on the ground in Takatori Station of JR-West (West Japan Railway Co.), which was involved in the 1995 South Hyogo Prefecture Earthquake, assuming Level 2 seismic motion ground of ground type II (G. Type II). The real time of the waveform was 20 s. The horizontal actuator is controlled by the external displacement (loading target displacement) input to the control computer (control PC) of the test machine. The loading target displacement in each step is obtained by a dynamic response analysis performed by the host computer (Host PC) or DSP. The Host PC and DSP are connected to the Ethernet, and the DSP and the control PC are connected via a terminal block using an analog I/O cable and BNC cable. The flow of the real-time hybrid simulation using DSP calculations is shown in Fig. 13.

Four loading velocities were used, 2 mm/s, 10 mm/s, 20 mm/s and real-time (hereinafter, RT). These loading velocities are the values until the horizontal actuator follows the loading target displacement of each step obtained by the Host PC or DSP calculations.

5.2 Real Time Hybrid Simulation Results

Figure 14 shows the results of a numerical analysis (hereinafter, analysis values) of the horizontal loading-series damper displacement relationship obtained in the hybrid experiment using the Host PC calculations. The values for horizontal loading consider the scale factor and sliding bearings. In RT loading, 300 s was required due to the effect of the time lag. The analysis values were calculated by using a hysteretic model approximated to the hysteresis curves obtained from unit experiments with the NES-D and LSD conducted in the past. As the loading velocity increased, the horizontal load asymptotically approached the analysis value. On the other hand, the displacement of the series damper tended to be larger than the analysis value. This is thought to occur because the displacement of the NES-D became larger than the analysis value due to the effect of the loading velocity.

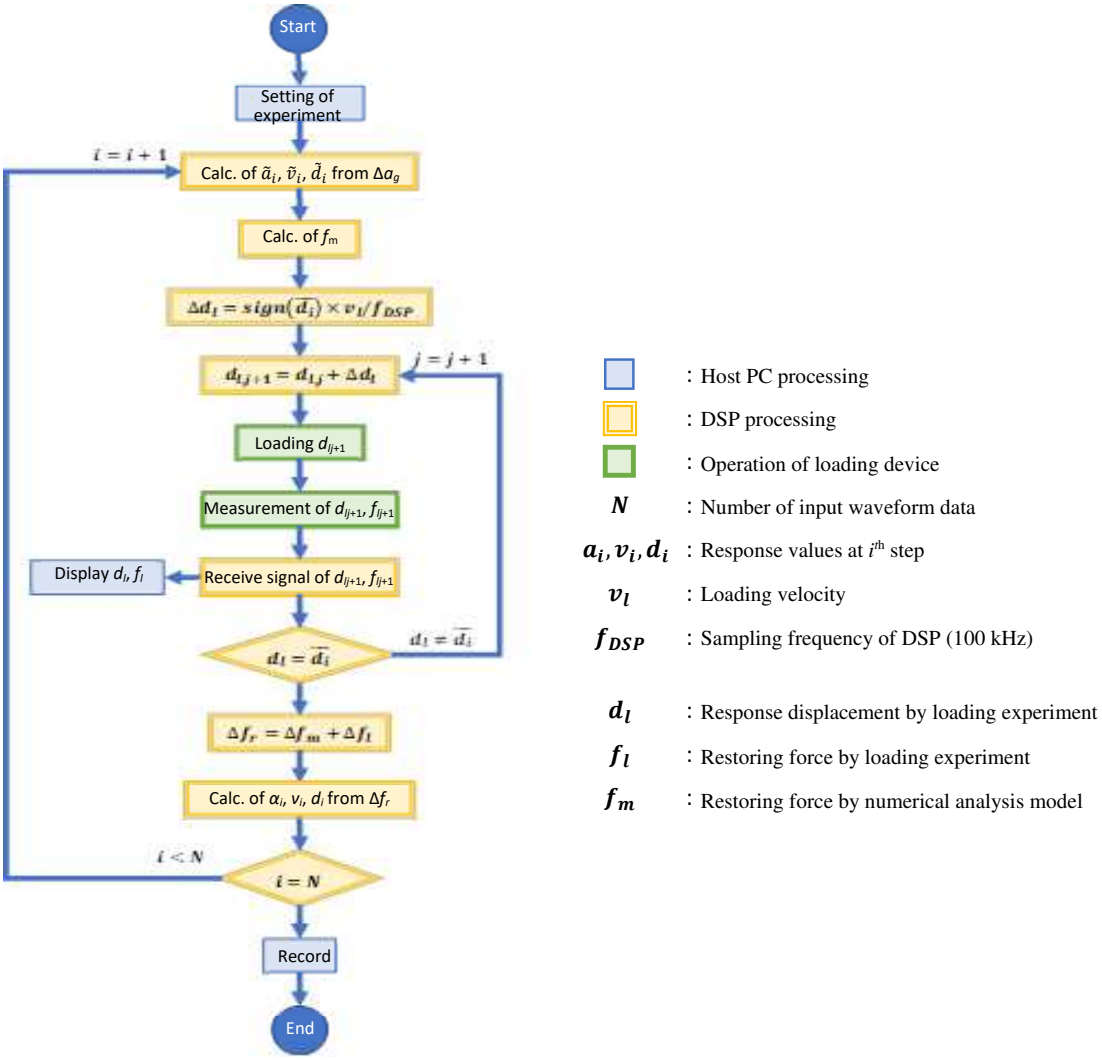

Fig. 13 – Flow of real-time hybrid simulation by DSP calculation

Figure 15(a) shows the horizontal loading-series damper displacement relationship obtained in the real-time hybrid simulation using DSP calculations with the analysis value. The maximum horizontal load, considering the scale factor and sliding bearings, is substantially equal to the analysis value. On the other hand, the displacement of the series damper is larger than the analysis value. As per the experiment with Host PC calculations, this is attributed to the effect of the displacement of the NES-D. It can be understood that the main displacement occurs in the LSD. Figure 15(c) shows the energy absorption ratio of the NES-D and LSD in comparison with the total energy absorption of the series damper. The energy absorption ratio of the LSD was 83 % of the total. Moreover, the experiment duration in the real-time hybrid simulation with DSP calculations was approximately 20 s, which is virtually identical with the time of the input waveform.

Figure 16 shows a comparison of the energy absorption ratios of the NES-D and LSD in the real-time hybrid simulation using the Host PC and DSP calculations. It can be understood that the energy absorption ratio of the LSD increases under faster loading velocities. Photo 3 shows the LSDs after RT loading. The response displacement of the LSD is larger than the analysis value, and in particular, under RT loading with DSP calculations, the color of the specimen changed due to the heat generated by the absorption of vibrational energy in the short span of 20 s.

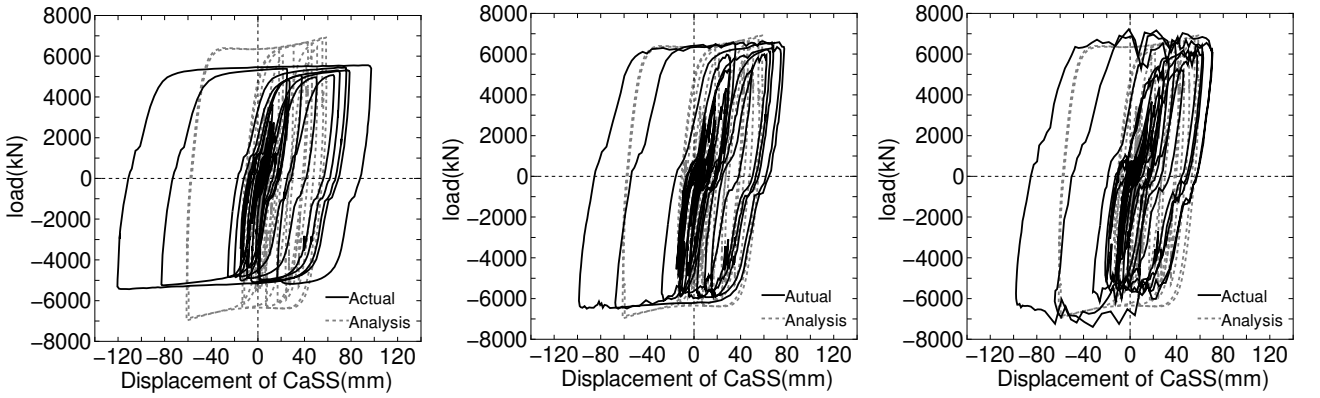

(a) Loading velocity 2 mm/s (b) Loading velocity 20 mm/s (c) RT loading (time lag occurred)

Fig. 14 – Results of real-time hybrid simulation with Host PC calculations

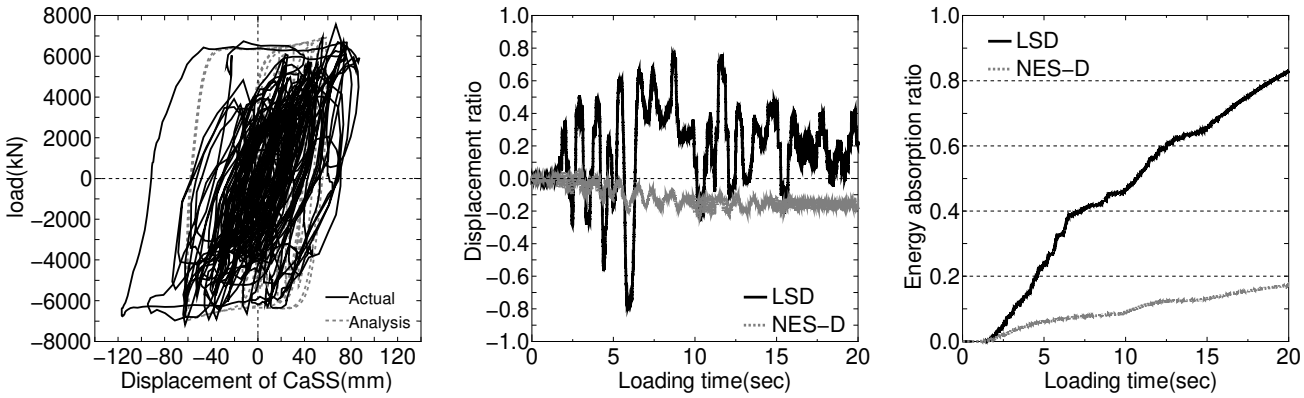

(a) RT loading (b) Displacement ratio (c) Energy absorption ratio

Fig. 15 – Results of real-time hybrid simulation with DSP calculations

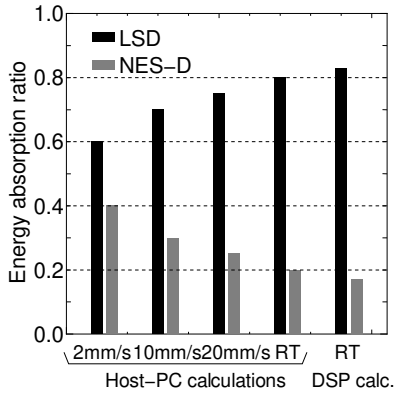

Fig. 16 – Comparison of energy absorption ratios (Host PC and DSP)

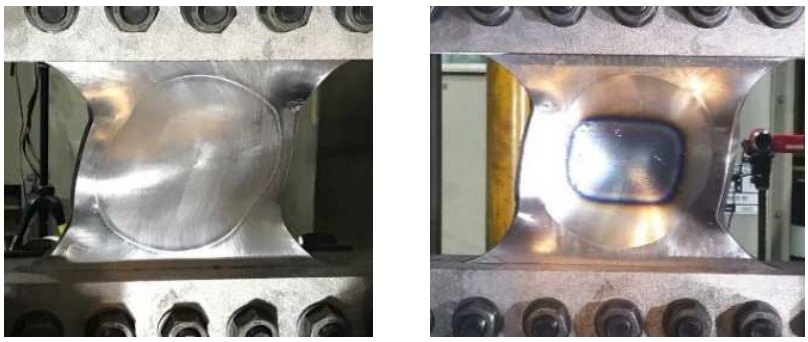

(a) Host PC calc. (300 s) (b) DSP calc. (20 s)

Photo 3 – LSD after RT loading

6. Conclusion

Focusing on bearings, where functions are concentrated, a performance confirmation experiment was conducted using a series damper combining an NES-D, which displays the displacement velocity dependency, and a steel LSD. This damper was proposed as a function-separated seismic isolation system from the viewpoints of anti-catastrophe performance and deterioration with age. The results obtained in this research are summarized below.

1) The possibility of separate action of the NES-D and the LSD was confirmed. Thus, this research showed that separating the device which follows deformation under normal conditions and the device that responds deformation during an earthquake is possible.
2) A real-time hybrid simulation system was constructed in order to study the seismic response characteristics of the whole isolated bridge, considering the actual earthquake seismic response of the series damper.
3) The horizontal load obtained in the experiment using Host PC calculations asymptotically approached the analysis value as the loading velocity increased. However, as the loading velocity decreased, the response displacement became larger than the analysis value due to the influence of the NES-D, which depends on the loading velocity.
4) The experiment duration under RT loading with DSP calculations was approximately 20 s, which is virtually identical to that of the input waveform. Although the maximum horizontal load was almost equal to the analysis value, the response displacement showed a tendency to be larger than the analysis value.
5) The energy absorption ratio of the LSD increased as the loading velocity became larger. The deformation ratio of the LSD also seemed to show a similar tendency.
6) Differences in the damage behavior of the LSD could be seen depending on the loading velocity. In the experiment with DSP calculations, the LSD showed discoloration due to a heat generation phenomenon.

7. Future Plan

The real-time hybrid simulation system with DSP calculations performed processing in substantially the same time as that of the input waveform demonstrated that simulation with high reproducibility of actual seismic response is possible. However, this research still considered a room for improvement on the reliability study technique, including improvements in the time lag of the hydraulic loading system, oscillation in real-time loading and other aspects. Based on this, the researchers planned to construct a correction function for the loading system employing a digital filter such as IIR, FIR or other type and identification of the loading system, and will also verify the seismic response characteristics of the series damper. [7].

8. References

[1] JSCE : Recommendations on Criteria for Seismic and Tsunami Resistant Performance for Nuclear Power Generation (Civil Engineering Viewpoint), 2013.7. (in Japanese)

[2] Riki Honda, Mitsuyoshi Akiyama, Shojiro Kataoka, Yoshikazu Takahashi, Atsushi Nozu, Yoshitaka Murono : Seismic Design Method to Consider “Anti-Catastrophe” Concept –A Study for Draft of Design-, Journal of JSCE A1, Vol.72, No.4, I_459-I_472, 2016. (in Japanese)

[3] Yuka Akiike, Ji Dang, Nobuhiro Yamazaki, Masayuki Ishiyama, Yuta Someya : Risk Mitigation Effect of Function Separated Bridges Under Design Limitation Exceeded Earthquakes, Journal of JSCE A1, Vol.74, No.4, I_955-I_963, 2018. (in Japanese)

[4] Nobuhiro Yamazaki, Takashi Harada, Masayuki Ishiyama, Seiya Matsumoto, Demin Feng, Satoshi Kanamori : Performance test of viscous cylinder damper, Japan Society of Civil Engineers 2014 Annual Meeting, I-069, pp.135-137, 2014.9. (in Japanese)

[5] Masayuki Ishiyama, Takashi Harada, Nobuhiro Yamazaki, Tatsumasa Takaku, Koji Imai, Tetsuhiko Aoki : Static performance of LENS type shear panel damper using low yield point steel, Japan Society of Civil Engineers 2009 Annual Meeting, I-042, pp.83-84, 2009.9. (in Japanese)

[6] Seiya Matsumoto, Takashi Harada, Masayuki Ishiyama, Nobuhiro Yamazaki, Demin Feng, Satoshi Kanamori : Durability test of viscous cylinder damper, Japan Society of Civil Engineers 2014 Annual Meeting, I-070, pp.137-138, 2014.9. (in Japanese)

[7] Akira Igarashi, Hirokazu Iemura, Hajime Tanaka : Development of substructure hybrid shake table test system and its application to performance verification of vibration control devices, Journal of structural engineering A, Vol.49, pp.281-288, 2003.3. (in Japanese)

